



Comparative analysis of Raman and IR spectra in LiCoPO_4 and LiNiPO_4 magnetoelectrics

A.V. Peschanskii¹, V.P. Gnezdilov¹, A.Yu. Glamazda^{1,2}

¹B. Verkin Institute for Low Temperature Physics and Engineering of the National Academy of Sciences of Ukraine, 47 Nauky Ave., 61103 Kharkov, Ukraine

²V.N. Karazin Kharkiv National University, 4 Svobody Sq., 61022, Kharkov, Ukraine

The olivine-type lithium orthophosphates LiMPO_4 ($M=\text{Fe}^{2+}$, Mn^{2+} , Co^{2+} , and Ni^{2+}) family have intriguing magnetoelectric properties, the entangled spin excitations and demonstrates a tight coupling of the phonon, electron, and magnetic subsystems. The present work is dedicated to the Raman studies of the LiCoPO_4 single crystal possessing the highest magnetoelectric coefficient among the above-mentioned crystals of the LiMPO_4 family. Raman spectroscopy is the non-destructive highly informative method that can simultaneously probe the phonon, electron, and magnetic excitations. In the present work, we discuss the electronic excitations of the Co^{2+} ion and additional phonon lines arising below $T_N = 21.9$ K.

Raman spectrum of the LiCoPO_4 single crystal was investigated in the frequency region of 3–1200 cm^{-1} in the temperature range between 5 and 300 K. A_g , B_{1g} , B_{2g} , and B_{3g} modes are active in Raman tensor components: A_g – XX , YY , ZZ , B_{1g} – XY , YX , B_{2g} – Z , ZX , and B_{3g} – YZ , ZY .

$X \parallel a$, $Y \parallel b$, $Z \parallel c$.

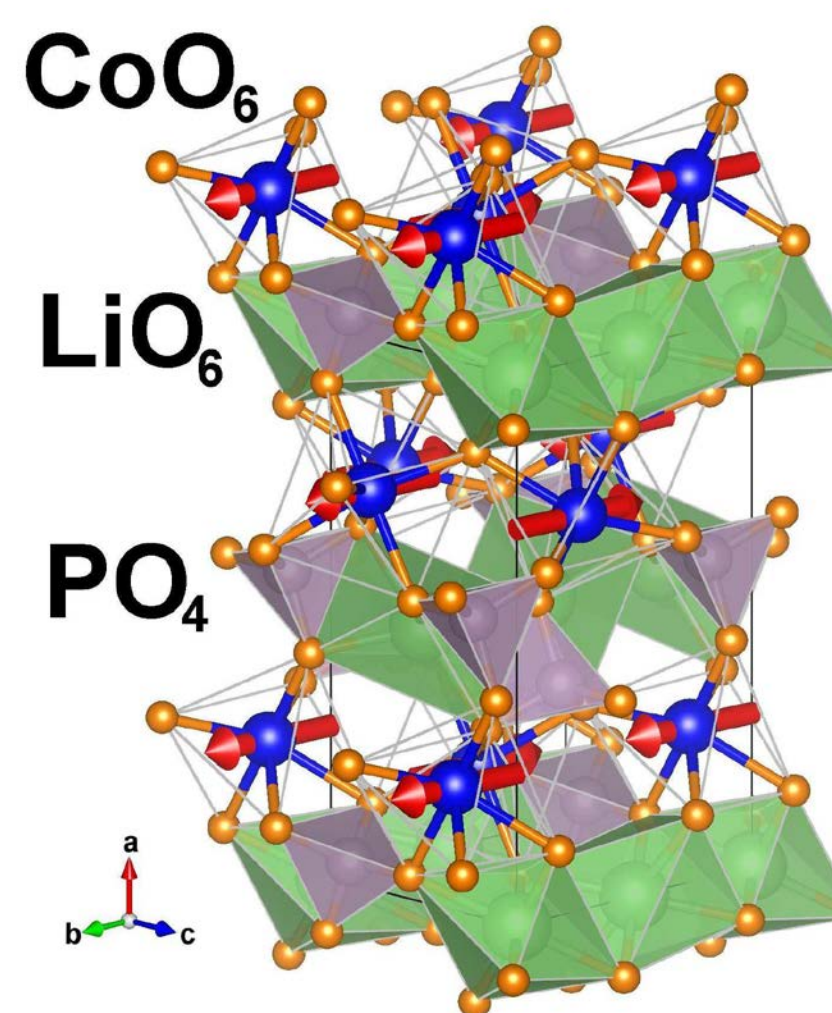


Fig. 1. Structure of LiCoPO_4 .

Structure of LiCoPO_4 : $Pnma$ (D_{2h}^{16}), $Z=4$, $a=10.092$ Å, $b=5.89$ Å, $c=4.705$ Å at $T=300$ K. $a=10.159$ Å, $b=5.9$ Å, $c=4.70$ Å at $T=8$ K.

$T_N = 21.9$ K, magnetic group $Pnma$ ($Z=4$).

Linear magnetoelectric (ME) – $P_i = \alpha_{ij} H_j$

ME coefficients:

$$|\alpha_{yx}| (4.2 \text{ K}) = 30.6 \text{ ps/m} \text{ and } |\alpha_{xy}| (4.2 \text{ K}) = 18.4 \text{ ps/m.}$$

$$\Gamma_{\text{vib}} = 11A_g + 7B_{1g} + 11B_{2g} + 7B_{3g} + 10A_u + 14B_{1u} + 10B_{2u} + 14B_{3u}$$

$$\Gamma_{\text{int}} = 6A_g + 3B_{1g} + 6B_{2g} + 3B_{3g} + 3A_u + 6B_{1u} + 3B_{2u} + 6B_{3u},$$

$$\Gamma_{\text{tr}} = 4A_g + 2B_{1g} + 4B_{2g} + 2B_{3g} + 5A_u + 6B_{1u} + 4B_{2u} + 6B_{3u},$$

$$\Gamma_{\text{lib}} = A_g + 2B_{1g} + B_{2g} + 2B_{3g} + 2A_u + B_{1u} + 2B_{2u} + B_{3u}.$$

$11A_g + 7B_{1g} + 11B_{2g} + 7B_{3g}$ modes are active in Raman spectra.

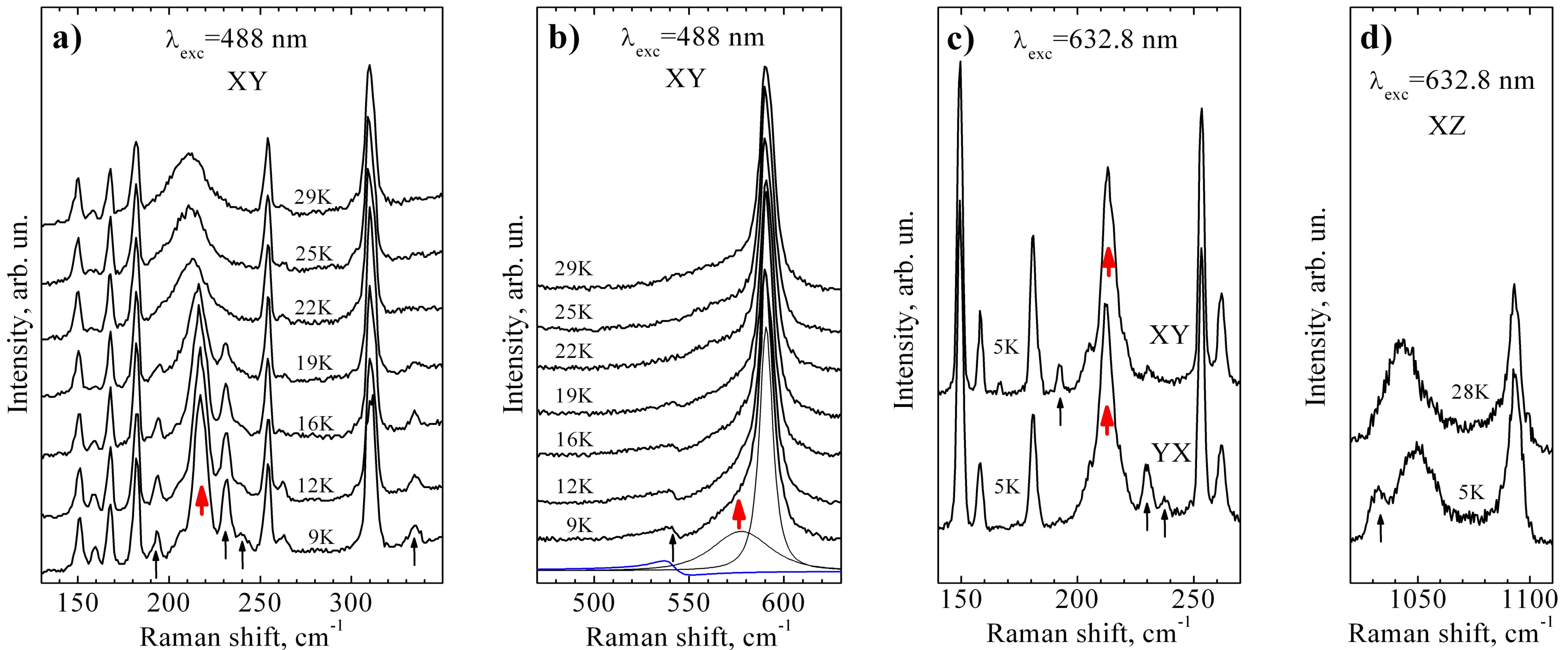


Fig. 2. Temperature dependent polarized Raman spectra taken in: a), b), c) – (YX, YX) B_{1g} ; d) – (XZ) B_{2g} modes. Spectral resolution: a), b) – 3.0 cm^{-1} ($\lambda_{\text{exc}} = 488 \text{ nm}$); c), d) – 1.8 cm^{-1} ($\lambda_{\text{exc}} = 632.8 \text{ nm}$). Thin black arrows are related to the additional phonon lines. The thick red arrows mark electronic excitations.

Frequency (in cm^{-1})			Factor-group symmetry	Site symmetry	Free PO_4 unit
Compound					
LiCoPO_4 [1]	LiNiPO_4 [2]	$\omega_{\text{Ni}} / \omega_{\text{Co}}$	D_{2h}^*	C_s	T_d
1093 (1087)	1090 (1088)	1.0009	B_{2g}	A'	
1080 (1077)	1074.5 (1072)	0.9954	A_g	(1080)	
1044 (1028)	1023 (1022.5)	0.9946	B_{2g}	A'	
1030 (1009)	1011.5 (1010.5)	1.0015	A_g	(1016)	
986 (986.5)	986 (987.5)	1.0010	B_{1g}	A''	
935 (943)	953 (952)	1.0095	B_{3g}	(970)	
—	—	—	B_{2g}	A'	
951 (951)	948.5 (948.5)	0.9974	A_g		
636 (634)	642 (640)	1.0095	A_g	A'	
596 (596)	603 (601)	1.0015	B_{2g}	(621)	
591 (590)	592.5 (591.5)	1.0025	B_{1g}	A''	
589.5 (589)	592 (591)	1.0034	B_{3g}	(591)	
577.5 (577)	581.5 (580)	1.0052	A_g	A'	
451 (449)	462.5 (459)	1.0223	A_g		
444.5 (448)	470.5 (467.5)	1.0435	B_{2g}	(455)	
433 (432)	442.5 (437)	1.0116	B_{3g}		
405 (401)	422.5 (417.5)	1.0411	B_{1g}	(427)	
279 (272)	308 (303.5)	1.1158			
261 (260)	287.5 (282.5)	1.0865			
216 (209)	242.5 (238)	1.1388			
157.5 (156)	175.5 (175)	1.1218			
104.5 (102)	114 (111.5)	1.0931			
310 (300.5)	325 (320.5)	1.0666			
253 (250.5)	258 (256)	1.0220			
181.5 (180)	199 (195)	1.0541			
149.5 (143)	—	—			
304.5 (299)	329.5 (325.5)	1.0886			
300 (299)	313 (310)	1.0368			
—	255.5 (252)	—			
166 (164)	182 (181.5)	1.1067			
151.5 (151)	172 (170)	1.1258			
323 (318.5)	329 (324.5)	1.0188			
248 (244.5)	262 (258.5)	1.0573			
174.5 (169)	193.5 (189)	1.1183			
113 (111)	122 (119.5)	1.0766			

External mode

Table 1. Symmetry and frequencies of the Raman phonon modes in LiCoPO_4 [1] and LiNiPO_4 [2] crystals at $T = 10$ K (300 K).

B_{1u}		B_{2u}		B_{3u}		LiCoPO_4 Exp. Raman line
LiNiPO_4 Exp. [3]	LiCoPO_4 Calc.	LiNiPO_4 Exp. [3]	LiCoPO_4 Calc.	LiNiPO_4 Exp. [3]	LiCoPO_4 Calc.	
196	183.3	202.3	189.4	165.2	154.5	192.2 XY
227	212.1			203.5	190.3	
259	242.2	236	221	-		230 YX
300	280.6	260	243.1	285	266.6	237.5 YX
311	290.9	356.6	333.5	313	292.7	333.5 XY
382	357.2	444	415.1	330.6	309.1	
-	-			363	339.4	
534	531.3	466	463.7	514	511.4	
581	578.1	543	540.3	580	577.1	541.2 XY
650	646.8			662.5	658.2	
-	-	951	946.3	942	937.3	
1083	1077.6			1035	1030	1031.5 XZ
1145	1139.3			1102	1096.5	

Table 2. Symmetry and frequencies of the experimental IR phonon modes in LiNiPO_4 [3] at $T = 30$ K and calculated IR phonon modes in LiCoPO_4 crystals (for calculations, the average frequency change coefficients were used for isomorphic substitution of Co by Ni: 1.07 for external and 1.005 for internal vibrational modes).

The performed analysis of taken Raman spectra in the different polarization configurations has revealed a number of additional phonon lines upon transition to a magnetically ordered state: 192.2, 230.0, 237.5, and 333.5 cm^{-1} (Figs. 1a, 1c); 541.4 cm^{-1} (Fig. 1b); 1031.5 cm^{-1} (Fig. 1d). A revealed effect can be explained in terms of two scenarios: 1) the unit-cell multiplication below T_N ; 2) IR phonon leakage due to the magneto-electric effect.

Conclusions

The assumption about the presence of the unit-cell multiplication contradicts the available X-ray and neutron diffraction data. There are no data on low-temperature IR phonons for LiCoPO_4 to verify the second scenario. The performed analysis of our Raman spectra of LiCoPO_4 [1] and LiNiPO_4 [2] allowed us to find the empirical dependences of the frequency positions of phonon lines on the ionic radius and atomic vibration types (Table 1). Having performed the comparative analysis of obtained abovementioned Raman data and IR spectra of LiNiPO_4 ($T=30$ K) [3], we calculated the frequency positions of the IR phonons in LiCoPO_4 . The results obtained are in good agreement with the frequency positions of additional phonons observed in Raman spectrum (Table 2).

References:

- [1] V. I. Fomin, V. P. Gnezdilov, V. S. Kurnosov, A. V. Peschanskii, et al., Low. Temp. Phys., 25, 829 (1999).
- [2] V. I. Fomin, V. P. Gnezdilov, V. S. Kurnosov, A. V. Peschanskii, et al., Low Temp. Phys. 28, 203 (2002).
- [3] M. S. Radionov, S. A. Klimin, A. Yu. Glamazda, A. V. Peschanskii, Low Temp. Phys. 48, 246 (2022).